



# Left ventricular deformation in the presence of left ventricular ‘rigid body rotation’ in healthy adults – three-dimensional speckle-tracking echocardiographic insights from the MAGYAR-Healthy Study

Attila Nemes, Árpád Kormányos, Nóra Ambrus, Csaba Lengyel

Department of Medicine, Albert Szent-Györgyi Medical School, University of Szeged, Hungary

*Contributions:* (I) Conception and design: A Nemes; (II) Administrative support: Á Kormányos, N Ambrus; (III) Provision of study materials or patients: A Nemes, Á Kormányos; (IV) Collection and assembly of data: Á Kormányos; (V) Data analysis and interpretation: Á Kormányos; (VI) Manuscript writing: All authors; (VII) Final approval of manuscript: All authors.

*Correspondence to:* Attila Nemes, MD, PhD, DSc. Department of Medicine, Albert Szent-Györgyi Medical School, University of Szeged, H-6725 Szeged, Semmelweis Street 8, Hungary. Email: nemes.attila@med.u-szeged.hu.

**Background:** During the heart cycle, the left ventricle (LV) not only shows a contraction-relaxation pattern, but LV has a rotational mechanics, as well. It is a known fact that certain pathologies may be associated with an absence of LV twist, when LV basal and apical regions rotate in the same clockwise (cw) or counterclockwise (ccw) direction called LV ‘rigid body rotation’ (LV-RBR), but it can also occur in healthy subjects. The present cohort study aimed to examine LV strains in healthy subjects with LV-RBR versus with normally directed LV rotational mechanics by three-dimensional speckle-tracking echocardiography (3DSTE).

**Methods:** The study consisted of 181 healthy individuals, from which 171 cases had normally directed LV rotational mechanics (mean age: 32.5±12.3 years, 79 males) and 10 healthy subject showed LV-RBR (mean age: 35.4±11.3 years, 3 males). Complete two-dimensional (2D) Doppler echocardiography and 3DSTE were performed in all healthy individuals.

**Results:** None of routine 2D Doppler echocardiographic parameters showed differences between the groups examined. There were no subjects with ≥ grade 1 regurgitation on any valves or with significant stenosis on any valves. 3DSTE-derived LV volumes, global and mean segmental strains did not differ between the groups examined. Apical anterior and lateral segments showed reduced segmental LV circumferential strain (CS) (−18.9%±8.5% vs. −26.7%±10.7%, P=0.02; −27.3%±12.6% vs. −34.8%±13.2%, P=0.08, respectively) and LV area strain (AS) (−26.8%±9.8% vs. −36.8%±12.0%, P=0.01; −35.7%±13.2% vs. −45.0%±14.6%) in healthy subjects having LV-RBR as compared to cases with normally directed LV rotational mechanics. These abnormalities were present only in subjects having cwLV-RBR.

**Conclusions:** Although global LV deformation is normal in the presence of LV-RBR in healthy adults, reduction of apical anterior and lateral LV-CS (and LV-AS) are present in cases with cwLV-RBR only suggesting segmental deformation abnormalities.

**Keywords:** Left ventricular (LV); rigid body rotation (RBR); strain; three-dimensional (3D); speckle-tracking

Submitted Jan 23, 2024. Accepted for publication May 15, 2024. Published online Jun 27, 2024.

doi: 10.21037/qims-24-140

View this article at: <https://dx.doi.org/10.21037/qims-24-140>

## Introduction

During the heart cycle, the left ventricle (LV) not only shows a deformation pattern (1-5), but due to its special myocardial architecture, LV has a rotational mechanics, as well with which its ejection can be optimized (6-10). In normal circumstances, LV base and apex rotate in opposite clockwise (cw) and counterclockwise (ccw) directions, respectively, their net difference is called LV twist, which is considered to be an important part of systolic function of the LV (6-10). It is a known fact that certain pathologies may be associated with an absence of LV twist, when LV basal and apical regions rotate in the same cw or ccw direction, which is called LV ‘rigid body rotation’ (LV-RBR), but it can also occur in healthy subjects (11). Among modern imaging methods, three-dimensional speckle-tracking echocardiography (3DSTE) is suitable not only for accurate LV volumetric measurements according to the heart cycle, but also for characterizing LV deformation with strains and determining LV rotational features at the same time using the same 3D virtual models ideal for physiologic studies (12-16). As the significance of LV-RBR on LV volumes and function are not deeply examined in real clinical settings in healthy subjects, the present cohort study aimed to examine 3DSTE-derived LV volumes and strains in healthy adults with normally directed LV rotational mechanics versus with LV-RBR. We present this article in accordance with the STROBE reporting checklist (available at <https://qims.amegroups.com/article/view/10.21037/qims-24-140/rc>).

## Methods

### Subjects

The study consisted of 181 healthy individuals, from which 171 cases had normally directed LV rotational mechanics (mean age: 32.5±12.3 years, 79 males) while 10 healthy subjects showed LV-RBR (mean age: 35.4±11.3 years, 3 males). None of the healthy subjects had any known diseases or pathological states, who were involved between 2011–2017. All of individuals underwent physical examination, laboratory assessments, standard 12-lead electrocardiography (ECG), two-dimensional (2D) Doppler echocardiography, and finally 3DSTE. All tests were negative, i.e. within the normal reference range. None of the subjects were athlete or had body mass index >30 kg/m<sup>2</sup>, or have taken medicines regularly. The analysis carried out in this study is part of the ‘Motion Analysis of the heart

and Great vessels by three-dimensional speckle-tracking echocardiography in Healthy subjects’ (MAGYAR-Healthy) Study, which has been organized to examine physiological relationships under healthy circumstances (‘Magyar’ means ‘Hungarian’ in Hungarian language). The study was conducted in accordance with the Declaration of Helsinki (as revised in 2013). Institutional and Regional Human Biomedical Research Committee at the University of Szeged, Hungary (No. 71/2011 and updated versions) approved the study. Informed consents were given by all subjects.

### 2D Doppler echocardiography

During the 2D echocardiographic studies, we followed the accepted professional guidelines. According to our practice, complete 2D echocardiographic examination was performed with Doppler analysis in all subjects first. During the tests, the participant was asked to lie on his left side, and then the heart was examined in the typical parasternal and apical views. Chamber quantifications were carried out in accordance with the guidelines including determination of LV ejection fraction (EF) by the Simpson’s method. Significant valvular stenoses and insufficiencies were excluded by Doppler echocardiography. Pulsed Doppler helped measurement of transmitral flow velocities in diastole and their ratio (E/A). For all analysis, Toshiba Artida™ echocardiography machine (Toshiba Medical Systems, Tokyo, Japan) was used in all healthy subjects attached to a PST-30BT (1–5 MHz) phased-array transducer (5).

### 3DSTE

Immediately after 2D echocardiographic examination, 3DSTE was performed (12-16). All 3DSTE analyses followed our standard protocol: firstly, in healthy subjects being in the left lateral decubitus position, 3D echocardiographic data acquisitions were performed from apical window following image optimisations (gain, magnitude, etc.) with the same Toshiba Artida™ echocardiographic tool (Toshiba Medical Systems, Tokyo, Japan), but using a 3D-capable a PST-25SX matrix-array transducer. ECG gating was used for all subjects who were in sinus rhythm, during 6 cardiac cycles, one wedge-shaped subvolume per cardiac cycle was acquired during to achieve the best image quality. The software stitched them together creating a pyramid-shaped full volume 3D

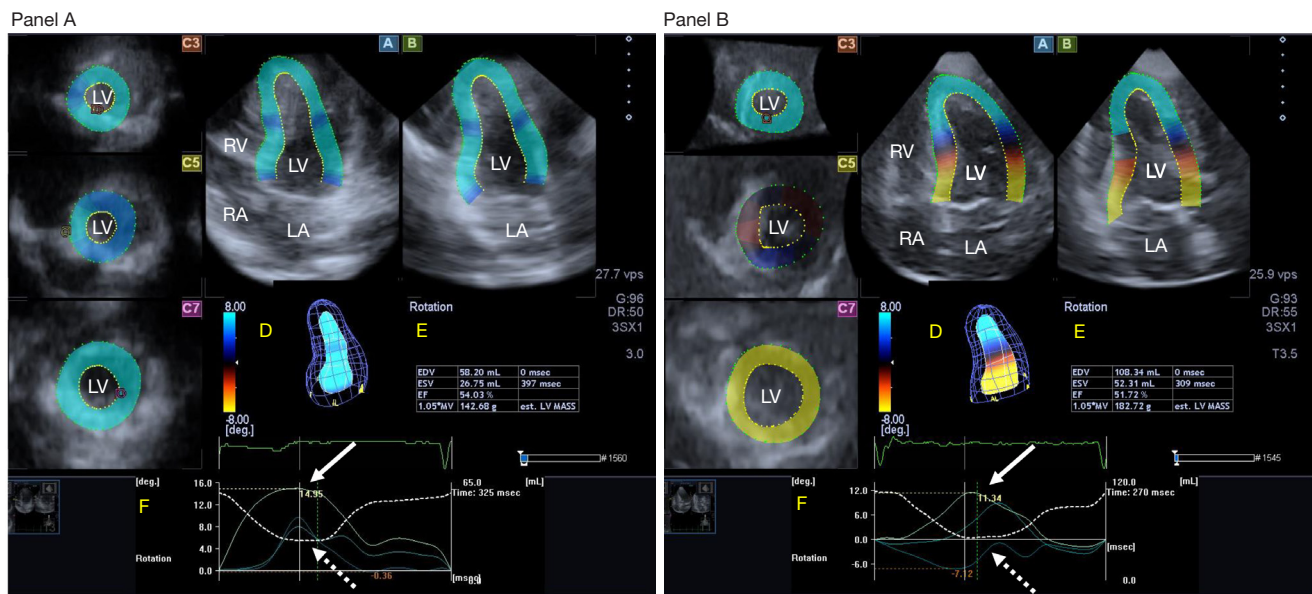


**Figure 1** Three-dimensional (3D) speckle-tracking echocardiography-derived assessment of the LV in a subject with LV rigid body rotation (Panel A) and in a case with normally directed LV rotational mechanics (Panel B): apical longitudinal four-chamber (A) and two-chamber views (B) and basal (C3), midventricular (C5) and apical (C7) short-axis views are shown together with 3D cast of the LV (D), volumetric LV parameters and LV ejection fraction (E). Time—LV volume changes (dashed white line) and time—apical (white arrow) and basal (dashed white arrow) LV rotations (F) are also presented. In Panel A both apical and basal LV rotations are in counterclockwise direction, while in Panel B, LV apical rotation is counterclockwise-directed, while LV basal rotation is clockwise-directed. LV, left ventricle; RV, right ventricle; LA, left atrium; RA, right atrium; EDV, end-diastolic volume; ESV, end-systolic volume; EF, ejection fraction; MV, mass volume.

echocardiographic dataset called ‘echocloud’.

Secondly, at a later date, 3D echocardiographic datasets were analysed offline with a 3D Wall Motion Tracking software (Ultra Extend, Toshiba Medical Systems, Tokyo, Japan, version 2.7, vendor-provided). The aim of the analysis was to create a 3D model/cast of the LV for same-time determination of LV strains and rotational mechanics. During the analysis, the software automatically created a five-division figure with apical longitudinal 4-chamber (AP4CH) and 2-chamber (AP2CH) views and basal, midventricular and apical cross-sectional views. For the creation of the LV 3D cast, septal and lateral mitral annulus (MA)-LV edges and apical endocardial surface of the LV were defined, then, a sequential analysis was performed (Figures 1,2).

Thirdly, using this 3D LV model, several functional LV properties were calculated:

- ❖ The following LV rotational parameters were provided: apical and basal LV rotations, LV twist (net sum of basal and apical LV rotations) and LV torsion (ratio of LV twist and LV length) (6-10).

- ❖ In case of LV-RBR, LV twist could not be calculated, only LV apico-basal gradient. In cwLV-RBR basal and apical LV regions rotate in the same cw direction (LV apex rotates in not-normal opposite direction), while in ccwLV-RBR in the same ccw direction (LV base rotates in not-normal opposite direction) (11).
- ❖ The following LV strain were measured (1-4):
  - ♦ LV area strain (LV-AS)—combination of LV-LS and LV-CS;
  - ♦ LV 3D strain (LV-3DS)—combination of LV-RS, LV-LS and LV-CS;
  - ♦ LV radial strain (LV-RS)—for characterizing thinning/thickening of the myocardial tissue;
  - ♦ LV longitudinal strain (LV-LS)—for characterizing lengthening/shortening of the myocardial tissue;
  - ♦ LV circumferential strain (LV-CS)—for characterizing widening/narrowing of the myocardial tissue.

Global (featuring the whole LV), segmental and mean segmental (calculated as the average of 16 segments) and regional (apical, midventricular and basal) LV strains were assessed.

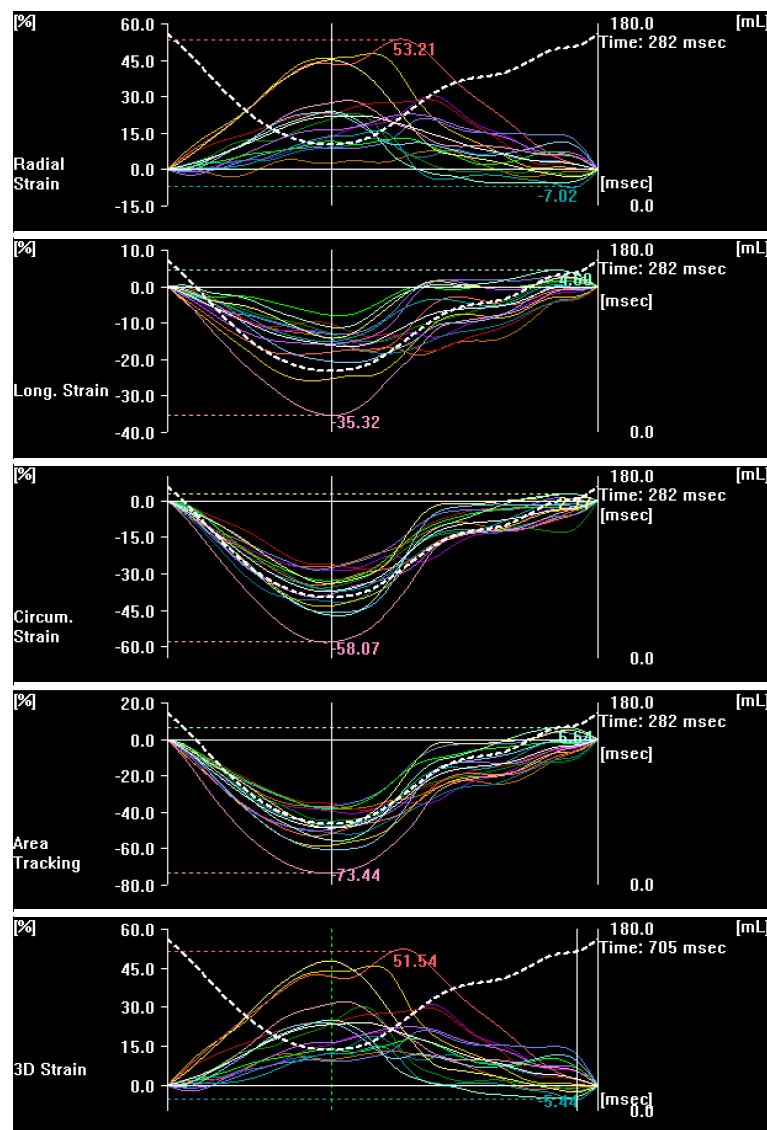


**Figure 2** 3D speckle-tracking echocardiography-derived assessment of left ventricular strains. Time—left ventricular volume changes (dashed white line) and time—global (white line) and segmental (coloured lines) radial, longitudinal, circumferential, area and three-dimensional strains are presented. 3D, three-dimensional.

### Statistical analysis

Mean  $\pm$  standard deviation and n (%) formats were used for data presentations, where appropriate. Significance was determined in case of P less than 0.05. Depending on data were continuous or categorical, Student's *t*-test, Bonferroni method following one-way analysis of variance (ANOVA) and Fischer's exact test were used, where appropriate. Statistical analyses were performed with SPSS version 22 (SPSS Inc., Michigan, IL, USA) software.

### Results

#### Clinical data

Systolic and diastolic blood pressures and heart rate were within the normal reference ranges ( $123.1 \pm 4.6$ ,  $73.4 \pm 3.9$  mmHg and  $70.4 \pm 2.1$  s<sup>-1</sup>, respectively). The mean height, weight and calculated body surface area and body mass index were also normal ( $171.3 \pm 7.3$  cm,  $72.0 \pm 10.2$  kg,  $1.83 \pm 0.11$  m<sup>2</sup> and  $24.2 \pm 2.1$  kg/m<sup>2</sup>). The subject population used for this manuscript is partly the same described in an

**Table 1** Clinical and two-dimensional echocardiography-derived parameters of healthy subjects showing normally directed left ventricular rotational mechanics versus left ventricular 'rigid body rotation'

Data	All healthy (n=181)	Normally directed LV rotational mechanics (n=171)	All LV-RBR (n=10)	ccwLV-RBR (n=5)	cwLV-RBR (n=5)
Age (years)	32.7±12.2	32.5±12.3	35.4±11.3	40.4±12.6	30.4±6.8
Male gender	81 [45]	79 [46]	3 [30]	0 [0]	3 [60]
LA (mm)	36.9±4.0	36.7±4.0	35.7±3.7	39.1±1.42	32.4±1.8*
LV-EDD (mm)	48.2±3.7	48.0±3.7	48.5±4.0	49.3±1.9	47.7±5.2
LV-EDV (mL)	107.4±25.7	106.4±22.8	112.6±22.7	121.1±14.3	104.0±26.1
LV-ESD (mm)	32.0±3.4	31.8±3.2	33.0±4.5	34.1±1.1	31.9±6.1
LV-ESV (mL)	37.1±10.4	36.2±8.9	40.7±11.9	44.0±5.5*	37.5±15.3
IVS (mm)	8.92±1.46	8.92±1.55	9.54±1.29	9.32±0.75	9.76±1.63
LV-PW (mm)	9.05±1.57	9.03±1.65	9.53±1.24	9.38±0.79	9.68±1.55
LV-EF (%)	65.8±4.6	66.0±4.9	64.4±5.5	63.6±2.6	65.2±7.2
E (cm)	82.0±17.7	80.5±17.4	76.6±18.2	70.2±13.0	83.0±20.3
A (cm)	64.4±18.5	65.2±19.9	54.2±9.9	54.6±11.3	53.9±8.2

Data are presented as number [percent] and mean ± standard deviation. \*, P<0.05 vs. normally directed LV rotational mechanics. LV, left ventricular; RBR, rigid body rotation; ccw, counterclockwise; cw, clockwise; LA, left atrial; EDD, end-diastolic diameter; EDV, end-diastolic volume; ESD, end-systolic diameter; ESV, end-systolic volume; IVS, interventricular septum; PW, posterior wall; EF, ejection fraction; E and A, early and late diastolic mitral inflow velocities.

early study from the MAGYAR-Healthy Study (17).

### 2D Doppler echocardiography

None of routine 2D Doppler echocardiographic parameters showed differences between the groups examined (Table 1). There were no subjects with ≥ grade 1 regurgitation on any valves or with significant stenosis on any valves. No wall motion abnormalities could be detected by visual assessment in any cases.

### 3DSTE

In subjects with normally directed LV rotational mechanics, LV twist proved to be 13.90±3.71 degrees, LV basal and apical rotations proved to be -4.26±2.09 degrees (ranging between -0.24 to -11.63 degrees) and 9.64±3.52 degrees (ranging between 3.17–21.95 degrees), respectively. Torsion proved to be 2.31±1.40 degree/cm. In the LV-RBR group, 5 individuals had cwLV-RBR with LV basal rotation -3.65±1.56 degrees (ranging between -1.85 to -6.12 degrees), LV apical rotation (-1.13±0.64 degrees, ranging between 0 to -1.71 degrees) and LV apico-basal gradient 4.78±1.52 degrees (ranging between 3.6–7.7 degrees), while 5 subjects showed ccwLV-RBR with LV basal rotation

0.74±0.34 degrees (ranging between 0–1.74 degrees), LV apical rotation 6.81±3.06 degrees (ranging between 3.22–11.94 degrees) and LV apico-basal gradient was 7.54±3.27 degrees, ranging 3.2–12.3 degrees, respectively). 3DSTE-derived LV volumes, global and mean segmental strains did not differ between that of healthy subjects having LV-RBR as compared to cases with normally directed LV rotational mechanics. However, reduced apical anterior and lateral segmental LV-CS and LV-area strain (AS) could be detected in the LV-RBR group. When cwLV-RBR and ccwLV-RBR cases were compared, these segmental abnormalities were present in cwLV-RBR subjects only with normal segmental pattern in ccwLV-RBR individuals. In ccwLV-RBR cases, no segmental LV strain abnormalities could be detected. Midventricular inferoseptal (MIS) LV segments showed significantly different LV-CS between LV-RBR groups (Tables 2–7).

### Discussion

The main engine of the circulatory system is LV, whose optimal pumping function is characterized by a complex pattern of deformation and twisting. In short, all to know about the structure of the LV is that fibers in the subepicardial side run in a left-handed direction,

**Table 2** Three-dimensional speckle-tracking echocardiography-derived LV volumes and global and mean segmental strains of healthy subjects showing normally directed LV rotational mechanics versus left ventricular ‘rigid body rotation’

Data	All healthy (n=181)	Normally directed LV rotational mechanics (n=171)	All LV-RBR (n=10)	ccwLV-RBR (n=5)	cwLV-RBR (n=5)
LV volumes					
LV-EDV (mL)	86.1±22.9	85.8±23.4	89.7±12.2	92.8±9.0	86.5±13.9
LV-ESV (mL)	36.2±10.5	36.1±10.7	39.3±6.2	40.0±5.5	38.6±6.8
LV-EF (%)	58.2±5.6	58.3±5.6	56.2±3.5	56.9±4.8	55.6±1.1
LV mass (g)	158.0±31.8	157.2±31.9	170.7±27.8	185.6±13.8	155.8±30.1*
LV strains					
LV-gRS	25.4±9.3	25.4±9.5	25.9±4.7	26.6±5.9	25.2±3.0
LV-gCS	-27.6±5.0	-27.7±5.1	-26.0±2.7	-27.2±3.1	-24.8±1.2
LV-gLS	-16.1±2.5	-16.1±2.5	-15.8±1.4	-15.5±1.3	-16.2±1.4
LV-g3DS	28.0±8.9	28.0±9.1	27.6±5.0	28.0±6.1	27.2±3.5
LV-gAS	-40.3±4.9	-40.4±5.0	-38.4±2.6	-39.1±3.4	-37.7±1.1
LV-msRS	27.7±8.8	27.7±9.0	27.7±4.7	28.6±5.6	26.8±3.2
LV-msCS	-28.5±4.8	-28.6±4.9	-26.9±2.5	-28.0±2.9	-25.8±1.1
LV-msLS	-16.9±2.4	-16.9±2.4	-16.5±1-5	-16.5±1.4	-16.5±1.7
LV-ms3DS	30.2±8.7	30.3±8.9	29.2±4.8	29.9±5.7	28.6±3.5
LV-msAS	-41.3±4.9	-41.4±5.0	-39.3±2.5	-40.2±3.1	-38.4±1.1

Data are presented as mean ± standard deviation. \*, P<0.05 vs. ccwLV-RBR. LV, left ventricular; RBR, rigid body rotation; ccw, counterclockwise; cw, clockwise; EDV, end-diastolic volume; ESV, end-systolic volume; EF, ejection fraction; g, global; RS, radial strain; CS, circumferential strain; LS, longitudinal strain; 3DS, three-dimensional strain; AS, area strain; ms, mean segmental.

**Table 3** Three-dimensional speckle-tracking echocardiography-derived LV segmental radial strains of healthy subjects showing normally directed LV rotational mechanics versus left ventricular ‘rigid body rotation’

Data	All healthy (n=181)	Normally directed LV rotational mechanics (n=171)	All LV-RBR (n=10)	ccwLV-RBR (n=5)	cwLV-RBR (n=5)
BA (%)	39.1±26.9	39.4±26.4	34.9±33.0	34.8±29.4	35.1±36.3
BAS (%)	39.4±20.7	39.6±20.8	37.2±19.8	37.0±23.1	37.4±15.7
BIS (%)	29.4±13.9	29.6±14.1	26.2±8.7	26.2±8.1	26.2±9.2
BI (%)	24.9±15.4	24.5±15.4	31.4±15.6	34.0±16.9	28.9±13.6
BIL (%)	27.0±19.5	26.7±19.4	31.8±21.2	29.9±26.3	33.7±14.2
BAL (%)	31.0±20.7	30.6±20.5	38.4±23.1	40.0±16.1	36.8±28.4
MA (%)	34.1±20.5	34.3±20.7	30.0±15.6	30.3±21.4	29.6±5.6
MAS (%)	37.1±16.8	36.9±17.2	40.6±7.9	41.5±8.9	39.6±6.7
MIS (%)	29.4±12.1	29.4±12.3	30.3±8.2	31.3±7.3	29.2±8.9
MI (%)	25.4±13.8	25.0±13.7	31.9±14.5	36.1±13.0	27.6±14.6
MIL (%)	25.8±17.7	25.7±17.7	27.2±18.2	28.5±20.4	26.0±15.5
MAL (%)	27.9±18.0	28.2±18.4	22.8±8.9	20.8±9.2	24.7±8.0
AA (%)	17.4±9.3	17.5±9.5	15.6±3.5	16.8±2.0	14.4±4.2
AS (%)	19.1±10.8	19.2±10.8	17.1±9.2	20.4±9.7	13.8±7.3
AI (%)	18.5±13.0	18.6±13.0	16.8±11.8	19.8±12.4	13.7±10.4
AL (%)	17.2±11.6	17.5±11.6	11.7±10.0	10.6±9.1	12.8±10.7

Data are presented as mean ± standard deviation. LV, left ventricular; RBR, rigid body rotation; ccw, counterclockwise; cw, clockwise; BA, basal anterior; BAS, basal anteroseptal; BIS, basal inferoseptal; BI, basal inferior; BIL, basal inferolateral; BAL, basal anterolateral; MA, midventricular anterior; MAS, midventricular anteroseptal; MIS, midventricular inferoseptal; MI, midventricular inferior; MIL, midventricular inferolateral; MAL, midventricular anterolateral; AA, apical anterior; AS, apical septal; AI, apical inferior; AL, apical lateral.

**Table 4** Three-dimensional speckle-tracking echocardiography-derived LV segmental circumferential strains of healthy subjects showing normally directed LV rotational mechanics versus left ventricular 'rigid body rotation'

Data	All healthy (n=181)	Normally directed LV rotational mechanics (n=171)	All LV-RBR (n=10)	ccwLV-RBR (n=5)	cwLV-RBR (n=5)
BA (%)	-26.6±10.9	-26.7±10.9	-24.8±11.8	-24.7±14.1	-25.0±9.0
BAS (%)	-26.4±9.6	-26.1±9.7	-30.4±7.1	-31.4±8.0	-29.4±5.9
BIS (%)	-25.6±10.0	-25.4±10.1	-27.6±9.0	-26.9±7.9	-28.4±9.9
BI (%)	-20.5±8.9	-20.3±8.8	-24.0±10.1	-21.7±12.5	-26.3±5.9
BIL (%)	-23.8±9.7	-23.8±9.8	-23.8±8.6	-22.0±8.1	-25.7±8.7
BAL (%)	-29.4±10.9	-29.5±11.1	-27.3±6.3	-24.6±4.4	-30.0±6.8
MA (%)	-29.9±9.9	-30.1±9.9	-25.0±8.0	-26.1±9.8	-23.9±5.3
MAS (%)	-28.1±9.2	-28.1±9.4	-28.1±6.9	-28.1±8.3	-28.2±5.0
MIS (%)	-29.4±9.8	-29.3±9.8	-31.0±9.2	-36.5±9.0	-25.5±5.3 <sup>†</sup>
MI (%)	-28.8±8.8	-28.9±8.9	-28.6±6.4	-25.5±6.8	-31.8±4.0
MIL (%)	-29.1±8.8	-29.2±8.9	-28.1±6.9	-30.2±6.2	-26.1±7.1
MAL (%)	-32.4±10.1	-32.6±10.2	-28.2±7.5	-31.2±5.5	-25.3±8.1
AA (%)	-26.3±10.7	-26.7±10.7	-18.9±8.5*	-20.2±5.1	-17.6±10.6*
AS (%)	-32.5±12.0	-32.7±12.1	-29.0±8.9	-33.3±10.7	-24.7±2.9
AI (%)	-33.3±12.0	-33.6±12.2	-28.6±7.1	-29.7±6.6	-27.5±7.4
AL (%)	-34.4±13.2	-34.8±13.2	-27.3±12.6	-36.9±10.3	-17.8±5.5*

Data are presented as mean ± standard deviation format. \*, P<0.05 vs. normally directed LV rotational mechanics; †, P<0.05 vs. ccwLV-RBR. LV, left ventricular; RBR, rigid body rotation; ccw, counterclockwise; cw, clockwise; BA, basal anterior; BAS, basal anteroseptal; BIS, basal inferoseptal; BI, basal inferior; BIL, basal inferolateral; BAL, basal anterolateral; MA, midventricular anterior; MAS, midventricular anteroseptal; MIS, midventricular inferoseptal; MI, midventricular inferior; MIL, midventricular inferolateral; MAL, midventricular anterolateral; AA, apical anterior; AS, apical septal; AI, apical inferior; AL, apical lateral.

in the middle layer run circumferentially, while in the subendocardial side run in a right-handed direction (17-22). The subendocardial and subepicardial contractions result in oppositely directed rotations, but due to larger rotational radius of the subepicardium and consequential greater torque, its rotation is expressed. According to these facts, the base of the LV rotates in cw direction, the apex of the LV rotates in ccw direction, thereby creating a so-called LV twist under healthy conditions. According to physiological studies, this form of LV muscle movement makes it possible that, despite the shortening of muscle fibers by 15–20%, the systolic LV-EF is normally 60–70% (6-10). However, it is important to know that at the same time LV thickens radially, shortens longitudinally and narrows circumferentially representing a special manifestation of LV deformation characterized by LV-RS (with positive signs), LV-LS and LV-CS (with negative signs), respectively with well-defined, but imaging method-dependent normal reference values (1-4).

Several clinical conditions can be accompanied with reduction of LV strains and rotational parameters (1,2,4,6-10). Moreover, in the presence of certain pathologies LV twist can be absent (11). The most frequently examined disorders are noncompaction cardiomyopathy, cardiac amyloidosis, acromegaly, etc., where its the absence of LV twist present in 25–100% of all cases and called as LV-RBR (11). In this condition, the base and apex of the LV rotate in the same cw or ccw direction having no LV twist, only LV apico-basal gradient in cw or ccw direction. In a recent study, about 5% of a healthy population showed LV-RBR (23). The objective of the present study was to find out, whether there are any difference between LV volumes and strains, when LV-RBR exists and when LV rotational mechanics are normal.

In recent decades, cardiac ultrasound has undergone tremendous development and new methods have become part of the daily routine. 3DSTE combines the advantages of speckle-tracking echocardiography and 3D

**Table 5** Three-dimensional speckle-tracking echocardiography-derived LV segmental longitudinal strains of healthy subjects showing normally directed LV rotational mechanics versus left ventricular 'rigid body rotation'

Data	All healthy (n=181)	Normally directed LV rotational mechanics (n=171)	All LV-RBR (n=10)	ccwLV-RBR (n=5)	cwLV-RBR (n=5)
BA (%)	-24.0±27.8	-24.0±7.7	-26.6±8.3	-27.5±8.3	-25.7±8.3
BAS (%)	-18.2±7.2	-18.2±7.2	-18.8±5.3	-19.7±5.6	-18.0±4.8
BIS (%)	-16.3±5.3	-16.4±5.4	-15.0±4.4	-15.5±5.2	-14.4±3.4
BI (%)	-17.9±5.8	-17.9±5.7	-17.8±7.0	-20.2±8.9	-15.3±2.8
BIL (%)	-19.3±7.6	-19.2±7.5	-20.7±7.8	-22.6±9.0	-18.8±5.8
BAL (%)	-23.9±7.9	-23.8±8.1	-25.9±5.2	-26.6±3.5	-25.2±6.5
MA (%)	-13.1±6.9	-13.1±7.0	-12.0±4.6	-10.9±4.9	-13.1±3.9
MAS (%)	-13.6±5.5	-13.6±5.6	-13.6±3.4	-13.2±3.9	-14.1±2.7
MIS (%)	-13.9±4.6	-14.0±4.7	-12.5±3.1	-13.9±3.0	-11.0±2.5
MI (%)	-13.9±4.8	-14.0±4.8	-13.0±4.7	-11.3±3.4	-14.7±5.3
MIL (%)	-12.6±5.4	-12.6±5.4	-11.8±6.5	-9.8±4.5	-13.9±7.5
MAL (%)	-14.3±6.1	-14.4±6.2	-12.6±5.3	-11.5±2.3	-13.8±7.0
AA (%)	-10.3±6.0	-10.5±6.1	-8.0±2.6	-8.3±3.0	-7.7±2.0
AS (%)	-22.9±7.6	-23.0±7.8	-21.8±3.8	-21.9±3.9	-21.7±3.8
AI (%)	-23.0±8.2	-23.0±8.2	-23.2±8.2	-21.0±6.7	-25.4±9.0
AL (%)	-13.0±6.9	-13.1±7.0	-11.3±6.1	-10.5±5.2	-12.1±6.8

Data are presented as mean ± standard deviation. LV, left ventricular; RBR, rigid body rotation; ccw, counterclockwise; cw, clockwise; BA, basal anterior; BAS, basal anteroseptal; BIS, basal inferoseptal; BI, basal inferior; BIL, basal inferolateral; BAL, basal anterolateral; MA, midventricular anterior; MAS, midventricular anteroseptal; MIS, midventricular inferoseptal; MI, midventricular inferior; MIL, midventricular inferolateral; MAL, midventricular anterolateral; AA, apical anterior; AS, apical septal; AI, apical inferior; AL, apical lateral.

echocardiography: with the help of virtually created 3D models of certain cardiac chambers, functional, strain and rotational parameters can be calculated in addition to accurate volumes respecting the cardiac cycle at the same time. In other words, in addition to measuring LV-EF, 3DSTE is also suitable for determination of LV rotational parameters and unidimensional/unidirectional LV-RS, LV-LS and LV-CS representing same direction contractility. Moreover, combined multidimensional/multidirectional strains such as LV-AS and LV-3DS can also be calculated (12-16). 3DSTE is validated for both volumetric, strain and rotational LV features (24-29) and their normal reference have already been published (23,30,31).

According to the presented findings it could be stated, that neither routine echocardiographic parameters, nor 3DSTE-derived LV volumes and global and mean segmental LV strains differ between healthy adults with normally directed LV rotational parameters versus subjects with LV-RBR. Although visual assessment did not confirm wall motion abnormalities in any cases, apical anterior and lateral LV-CS

(and consequential LV-AS) reduction could be detected in subjects with LV-RBR. These segmental LV strain reductions were present only in cases presenting cwLV-RBR, when normally ccw apical LV rotation was reversed. In subjects with ccwLV-RBR (when normally cw basal LV rotation was reversed) no segmental LV deformation abnormalities could be detected. Moreover, differences in certain segmental LV-CS were also present between these subgroups.

It cannot be known for certain about the reasons for why healthy individuals show LV-RBR, its clinical significance is also not clear. Although it was tried to rule out the presence of possible pathological processes as much as possible in all cases, it could not be ruled it out unequivocally. Myocardial-architectural abnormalities or unusual/not universally characterized myocardial arrangement can only arise as a theoretical possibility, but the existence of latently existing asymptomatic diseases cannot be ruled out either (6-11). Therefore, follow-up studies with larger healthy populations are warranted to confirm presented findings. Moreover, in addition to the above, an even more detailed



**Table 6** Three-dimensional speckle-tracking echocardiography-derived LV segmental three-dimensional strains of healthy subjects showing normally directed LV rotational mechanics versus left ventricular ‘rigid body rotation’

Data	All healthy (n=181)	Normally directed LV rotational mechanics (n=171)	All LV-RBR (n=10)	ccwLV-RBR (n=5)	cwLV-RBR (n=5)
BA (%)	41.1±26.5	41.4±26.1	36.7±31.9	34.5±29.3	38.9±34.1
BAS (%)	41.0±20.1	41.2±20.2	38.0±18.5	38.2±20.9	37.9±15.7
BIS (%)	30.4±13.5	30.7±13.7	26.7±8.8	26.9±7.6	26.5±9.8
BI (%)	28.9±14.7	28.6±14.6	34.0±16.0	36.4±15.9	31.7±15.8
BIL (%)	34.5±18.2	34.2±18.0	40.5±19.2	37.4±21.7	43.5±15.8
BAL (%)	35.0±19.6	34.7±19.4	39.6±22.2	39.1±17.9	40.1±25.8
MA (%)	34.8±20.1	35.1±20.3	29.8±16.0	29.8±21.9	30.0±5.5
MAS (%)	38.0±16.7	37.9±17.0	40.2±9.3	42.2±11.1	38.3±6.4
MIS (%)	30.7±12.0	30.6±12.1	31.6±10.3	34.3±10.9	28.9±8.9
MI (%)	26.9±13.6	26.6±13.5	32.1±14.4	36.2±13.1	28.0±14.5
MIL (%)	28.8±17.0	28.7±16.8	30.0±18.8	29.9±18.2	30.1±19.3
MAL (%)	29.7±17.9	30.0±18.2	24.7±9.9	20.6±6.9	28.7±10.7
AA (%)	18.4±10.0	18.6±10.2	16.1±3.6	18.0±1.5	14.2±4.1
AS (%)	21.2±11.6	21.4±11.6	17.9±10.1	21.8±10.8	13.9±7.5
AI (%)	20.5±13.4	20.7±13.5	17.5±12.1	21.1±12.7	13.9±10.4
AL (%)	19.0±12.0	19.4±12.0	12.4±9.3	11.5±9.3	13.2±9.2

Data are presented as mean ± standard deviation. LV, left ventricular; RBR, rigid body rotation; ccw, counterclockwise; cw, clockwise; BA, basal anterior; BAS, basal anteroseptal; BIS, basal inferoseptal; BI, basal inferior; BIL, basal inferolateral; BAL, basal anterolateral; MA, midventricular anterior; MAS, midventricular anteroseptal; MIS, midventricular inferoseptal; MI, midventricular inferior; MIL, midventricular inferolateral; MAL, midventricular anterolateral; AA, apical anterior; AS, apical septal; AI, apical inferior; AL, apical lateral.

analysis of the clinical significance of LV-RBR in different pathologies would be interesting.

### Limitation section

The following important limitations should be considered when interpreting results of this study:

- ❖ As detailed above, subclinical pathology may have existed in some cases, as participants considered themselves healthy and no laboratory and imaging tests were carried out that seemed unnecessary.
- ❖ The biggest drawback of 3DSTE is its image quality, which is known to be worse than routine 2D echocardiography.
- ❖ The most well-known sources of error including the followings: it takes 4–6 heart cycles to acquire 3D datasets, then software switch subvolumes together. In this case, the movement of the patient or transducer can significantly affect image quality. In addition, respiratory movement and arrhythmias

may affect image quality as well.

- ❖ The present study only aimed to analyze LV, although 3DSTE would have been suitable for detailed analysis of other heart cavities as well.
- ❖ It was not aimed to validate 3DSTE-derived LV strains representing deformation and rotational parameters due to their validated nature.
- ❖ The ventricular septum was considered part of the LV in the present study, although it could be debated which chamber it is part of.
- ❖ In the present study, only the relationship between LV strain and rotational parameters defined by 3DSTE was examined. We did not consider it the goal to present other morphological abnormalities of LV, to measure the diameter or areas of LV in a particular selected plane, nor to analyse regional strains and rotational parameters of LV.
- ❖ Only 10 healthy cases with confirmed LV-RBR were involved into the present study. However, literature data regarding to the exact ratio of such cases in a

**Table 7** Three-dimensional speckle-tracking echocardiography-derived LV segmental area strains of healthy subjects showing normally directed LV rotational mechanics versus left ventricular 'rigid body rotation'

Data	All healthy (n=181)	Normally directed LV rotational mechanics (n=171)	LV-RBR (n=10)	ccwLV-RBR (n=5)	cwLV-RBR (n=5)
BA (%)	-43.3±11.0	-43.3±10.9	-44.4±11.5	-45.6±12.4	-43.2±10.4
BAS (%)	-40.0±10.4	-39.4±10.5	-43.6±7.3	-45.0±7.7	-42.3±6.6
BIS (%)	-37.4±10.4	-37.4±10.5	-38.1±8.0	-37.8±9.2	-38.4±6.5
BI (%)	-34.6±8.8	-34.4±8.7	-37.3±11.1	-36.7±15.0	-38.0±4.9
BIL (%)	-38.2±10.7	-38.1±10.7	-39.3±11.6	-39.0±12.6	-39.7±10.6
BAL (%)	-45.6±10.8	-45.6±11.1	-45.9±5.4	-44.1±5.7	-47.8±4.3
MA (%)	-39.6±11.6	-39.9±11.7	-34.4±8.5	-33.9±10.8	-34.8±5.3
MAS (%)	-40.6±9.6	-40.6±9.8	-39.3±7.3	-39.0±9.4	-39.6±4.3
MIS (%)	-39.7±10.0	-39.7±10.1	-39.7±8.6	-45.4±7.6	-34.1±5.2 <sup>†</sup>
MI (%)	-38.8±8.6	-38.9±10.1	-37.7±7.1	-33.9±7.2	-41.5±4.5
MIL (%)	-38.5±8.9	-38.5±9.1	-37.4±8.1	-37.0±5.2	-37.9±6.9
MAL (%)	-42.9±10.4	-43.2±10.5	-37.9±8.3	-39.6±4.2	-36.2±10.7
AA (%)	-36.3±12.1	-36.8±12.0	-26.8±9.8*	-28.7±4.7	-25.0±12.7*
AS (%)	-49.5±13.4	-49.7±13.6	-45.6±9.0	-48.9±10.7	-42.4±5.2
AI (%)	-48.9±13.3	-49.1±13.5	-45.1±9.4	-44.7±9.3	-45.5±9.4
AL (%)	-44.4±14.7	-45.0±14.6	-35.7±13.2*	-43.7±13.3	-27.7±6.8* <sup>†</sup>

Data are presented as mean ± standard deviation. \*, P<0.05 vs. normally directed LV rotational mechanics; †, P<0.05 vs. ccwLV-RBR. LV, left ventricular; RBR, rigid body rotation; ccw, counterclockwise; cw, clockwise; BA, basal anterior; BAS, basal anteroseptal; BIS, basal inferoseptal; BI, basal inferior; BIL, basal inferolateral; BAL, basal anterolateral; MA, midventricular anterior; MAS, midventricular anteroseptal; MIS, midventricular inferoseptal; MI, midventricular inferior; MIL, midventricular inferolateral; MAL, midventricular anterolateral; AA, apical anterior; AS, apical septal; AI, apical inferior; AL, apical lateral.

healthy population is limited.

- ❖ Only minor abnormalities could be detected following analysis of the data. However, there were no studies in the literature, which even used conventional methods in a such rare situation in healthy adults. It is true that clinical significance of findings is questionable. However, it is believed, that understanding myocardial mechanics even in healthy subjects can have relevance.

## Conclusions

Although global LV deformation is normal in the presence of LV-RBR in healthy adults, anterior and lateral apical LV-CS (and LV-AS) reduction are present suggesting segmental deformation abnormalities.

## Acknowledgments

*Funding:* None.

## Footnote

*Reporting Checklist:* The authors have completed the STROBE reporting checklist. Available at <https://qims.amegroups.com/article/view/10.21037/qims-24-140/rc>

*Conflicts of Interest:* All authors have completed the ICMJE uniform disclosure form (available at <https://qims.amegroups.com/article/view/10.21037/qims-24-140/coif>). A.N. serves as an unpaid editorial board member of *Quantitative Imaging in Medicine and Surgery*. The other authors have no conflicts of interest to declare.

*Ethical Statement:* The authors are accountable for all aspects of the work in ensuring that questions related to the accuracy or integrity of any part of the work are appropriately investigated and resolved. The study was conducted in accordance with the Declaration of Helsinki (as revised in 2013). The study was approved by the Institutional and Regional Human Biomedical Research

Committee of University of Szeged (Hungary) (No. 71/2011 and updated versions), and informed consent was taken from all subjects.

*Open Access Statement:* This is an Open Access article distributed in accordance with the Creative Commons Attribution-NonCommercial-NoDerivs 4.0 International License (CC BY-NC-ND 4.0), which permits the non-commercial replication and distribution of the article with the strict proviso that no changes or edits are made and the original work is properly cited (including links to both the formal publication through the relevant DOI and the license). See: <https://creativecommons.org/licenses/by-nc-nd/4.0/>.

## References

- Meyers BA, Brindise MC, Kutty S, Vlachos PP. A method for direct estimation of left ventricular global longitudinal strain rate from echocardiograms. *Sci Rep* 2022;12:4008.
- Narang A, Addetia K. An introduction to left ventricular strain. *Curr Opin Cardiol* 2018;33:455-63.
- Voigt JU, Pedrizzetti G, Lysyansky P, Marwick TH, Houle H, Baumann R, Pedri S, Ito Y, Abe Y, Metz S, Song JH, Hamilton J, Sengupta PP, Kolias TJ, d'Hooge J, Aurigemma GP, Thomas JD, Badano LP. Definitions for a common standard for 2D speckle tracking echocardiography: consensus document of the EACVI/ASE/Industry Task Force to standardize deformation imaging. *Eur Heart J Cardiovasc Imaging* 2015;16:1-11.
- Edvardsen T, Klæboe LG. Imaging and heart failure: myocardial strain. *Curr Opin Cardiol* 2019;34:490-4.
- Lang RM, Badano LP, Mor-Avi V, Afilalo J, Armstrong A, Ernande L, Flachskampf FA, Foster E, Goldstein SA, Kuznetsova T, Lancellotti P, Muraru D, Picard MH, Rietzschel ER, Rudski L, Spencer KT, Tsang W, Voigt JU. Recommendations for cardiac chamber quantification by echocardiography in adults: an update from the American Society of Echocardiography and the European Association of Cardiovascular Imaging. *Eur Heart J Cardiovasc Imaging* 2015;16:233-70.
- Bloechlinger S, Grander W, Bryner J, Dünser MW. Left ventricular rotation: a neglected aspect of the cardiac cycle. *Intensive Care Med* 2011;37:156-63.
- Omar AMS, Vallabhajosyula S, Sengupta PP. Left ventricular twist and torsion: research observations and clinical applications. *Circ Cardiovasc Imaging* 2015;8:e003029.
- Nakatani S. Left ventricular rotation and twist: why should we learn? *J Cardiovasc Ultrasound* 2011;19:1-6.
- Sengupta PP, Tajik AJ, Chandrasekaran K, Khandheria BK. Twist mechanics of the left ventricle: principles and application. *JACC Cardiovasc Imaging* 2008;1:366-76.
- Stöhr EJ, Shave RE, Baggish AL, Weiner RB. Left ventricular twist mechanics in the context of normal physiology and cardiovascular disease: a review of studies using speckle tracking echocardiography. *Am J Physiol Heart Circ Physiol* 2016;311:H633-44.
- Nemes A, Kormányos Á. Prevalence of left ventricular 'rigid body rotation', the near absence of left ventricular twist (insights from the MAGYAR studies). *Rev Cardiovasc Med* 2022;23:5.
- Nabeshima Y, Seo Y, Takeuchi M. A review of current trends in three-dimensional analysis of left ventricular myocardial strain. *Cardiovasc Ultrasound* 2020;18:23.
- Ammar KA, Paterick TE, Khandheria BK, Jan MF, Kramer C, Umland MM, Tercius AJ, Baratta L, Tajik AJ. Myocardial mechanics: understanding and applying three-dimensional speckle tracking echocardiography in clinical practice. *Echocardiography* 2012;29:861-72.
- Urbano-Moral JA, Patel AR, Maron MS, Arias-Godinez JA, Pandian NG. Three-dimensional speckle-tracking echocardiography: methodological aspects and clinical potential. *Echocardiography* 2012;29:997-1010.
- Muraru D, Niero A, Rodriguez-Zanella H, Cherata D, Badano L. Three-dimensional speckle-tracking echocardiography: benefits and limitations of integrating myocardial mechanics with three-dimensional imaging. *Cardiovasc Diagn Ther* 2018;8:101-17.
- Seo Y, Ishizu T, Atsumi A, Kawamura R, Aonuma K. Three-dimensional speckle tracking echocardiography. *Circ J* 2014;78:1290-301.
- Buckberg GD. Basic science review: the helix and the heart. *J Thorac Cardiovasc Surg* 2002;124:863-83.
- Armour JA, Randall WC. Structural basis for cardiac function. *Am J Physiol* 1970;218:1517-23.
- Greenbaum RA, Ho SY, Gibson DG, Becker AE, Anderson RH. Left ventricular fibre architecture in man. *Br Heart J* 1981;45:248-63.
- Sengupta PP, Korinek J, Belohlavek M, Narula J, Vannan MA, Jahangir A, Khandheria BK. Left ventricular structure and function: basic science for cardiac imaging. *J Am Coll Cardiol* 2006;48:1988-2001.
- Torrent-Guasp F, Buckberg GD, Clemente C, Cox JL, Coghlan HC, Gharib M. The structure and function of the helical heart and its buttress wrapping. I. The normal macroscopic structure of the heart. *Semin Thorac*

- Cardiovasc Surg 2001;13:301-19.
22. Torrent-Guasp F, Kocica MJ, Corno AF, Komeda M, Carreras-Costa F, Flotats A, Cosin-Aguillar J, Wen H. Towards new understanding of the heart structure and function. *Eur J Cardiothorac Surg* 2005;27:191-201.
  23. Kormányos Á, Kalapos A, Domsik P, Lengyel C, Forster T, Nemes A. Normal values of left ventricular rotational parameters in healthy adults—Insights from the three-dimensional speckle tracking echocardiographic MAGYAR-Healthy Study. *Echocardiography* 2019;36:714-21.
  24. Nesser HJ, Mor-Avi V, Gorissen W, Weinert L, Steringer-Mascherbauer R, Niel J, Sugeng L, Lang RM. Quantification of left ventricular volumes using three-dimensional echocardiographic speckle tracking: comparison with MRI. *Eur Heart J* 2009;30:1565-73.
  25. Kleijn SA, Brouwer WP, Aly MFA, Rüssel IK, de Roest GJ, Beek AM, van Rossum AC, Kamp O. Comparison between three-dimensional speckle-tracking echocardiography and cardiac magnetic resonance imaging for quantification of left ventricular volumes and function. *Eur Heart J Cardiovasc Imaging* 2012;13:834-9.
  26. Kleijn SA, Aly MFA, Terwee CB, van Rossum AC, Kamp O. Reliability of left ventricular volumes and function measurements using three-dimensional speckle tracking echocardiography. *Eur Heart J Cardiovasc Imaging* 2012;13:159-68.
  27. Ashraf M, Myronenko A, Nguyen T, Inage A, Smith W, Lowe RI, Thiele K, Gibbons Kroeker CA, Tyberg JV, Smallhorn JF, Sahn DJ, Song X. Defining left ventricular apex-to-base twist mechanics computed from high-resolution 3D echocardiography: validation against sonomicrometry. *JACC Cardiovasc Imaging* 2010;3:227-34.
  28. Zhou Z, Ashraf M, Hu D, Dai X, Xu Y, Kenny B, Cameron B, Nguyen T, Xiong L, Sahn DJ. Three-dimensional speckle-tracking imaging for left ventricular rotation measurement: an in vitro validation study. *J Ultrasound Med* 2010;29:903-9.
  29. Andrade J, Cortez LD, Campos O, Arruda AL, Pinheiro J, Vulcanis L, Shiratsuchi TS, Kalil-Filho R, Cerri GG. Left ventricular twist: comparison between two- and three-dimensional speckle-tracking echocardiography in healthy volunteers. *Eur J Echocardiogr* 2011;12:76-9.
  30. Kormányos Á, Kalapos A, Domsik P, Gyenes N, Lengyel C, Nemes A. Normal reference values of left ventricular volumetric parameters in healthy adults—real-life single-center experience from the three-dimensional speckle-tracking echocardiographic MAGYAR-Healthy Study. *Quant Imaging Med Surg* 2021;11:1496-503.
  31. Nemes A, Kormányos Á, Kalapos A, Domsik P, Gyenes N, Ambrus N, Lengyel C. Normal reference values of left ventricular strain parameters in healthy adults: Real-life experience from the single-center three-dimensional speckle-tracking echocardiographic MAGYAR-Healthy Study. *J Clin Ultrasound* 2021;49:368-77.

**Cite this article as:** Nemes A, Kormányos Á, Ambrus N, Lengyel C. Left ventricular deformation in the presence of left ventricular ‘rigid body rotation’ in healthy adults—three-dimensional speckle-tracking echocardiographic insights from the MAGYAR-Healthy Study. *Quant Imaging Med Surg* 2024;14(7):4605-4616. doi: 10.21037/qims-24-140